Variation of soluble and insoluble calcium in red rains related to dust sources and transport patterns from North Africa to northeastern Spain

A. Avila,[1] M. Alarcón,[2] S. Castillo,[3] M. Escudero,[1,4] J. García Orellana,[5] P. Masqué,[5] and X. Querol[3]

Received 2 February 2006; revised 11 August 2006; accepted 26 September 2006; published 13 March 2007.

[1] We use the chemical composition of African dust delivered by red rains at a rural site in northeastern Spain (Montseny, 41°46′N, 2°21′E) to describe its relationship with the possible provenance areas and the processes occurring during transport. To this end, we obtained the red rain insoluble composition for the major elements (Al, Fe, Ca, Mg, K, P, Ti, and Na) in 30 filters, the ^{210}Pb concentration in 23 filters, and the soluble cation concentrations (Na, K, Ca, and Mg) in 28 coincident red rain samples. These samples comprised most major events occurring at the site from 1983 to 2002. On the basis of back trajectories and satellite images, a distinction has been made between an eastern and western air mass flux with respect to 0° Greenwich for the analyzed samples. Principal component and ANOVA analyses between the two provenance groups have shown striking differences in the insoluble phase, with eastern samples being significantly richer in insoluble Ca, Mg, and Sr compared to western samples. Conversely, western samples had significantly higher concentrations of insoluble Al, Fe, K, V, and ^{210}Pb than eastern samples. Therefore, in the insoluble phase, the ratios of various elements to Ca were significantly higher in western provenances. However, these differences disappeared when considering bulk Ca ratios (bulk Ca = insoluble + soluble Ca). Neither of the ratios Fe/Al and Ti/Fe showed significant differences. This lack of differences is interpreted in view of a similar carbonated lithology broadly underlying both areas. The difference in insoluble Ca with respect to total Ca between provenances ($Ca_{insoluble}/Ca_{total}$ = 0.10 and 0.70 for western and eastern trajectories, respectively) is interpreted as a difference in calcite dissolution during transport. Evidence from ^{210}Pb data and from the length of the back trajectories indicates that western trajectories covered a longer distance than the eastern ones; their higher soluble Ca could be due to (1) higher calcite dissolution due to longer contact with wet fronts from the Atlantic and (2) particle segregation during transport, with finer (carbonate) particles more prone to dissolution due to a higher surface to volume ratio.

Citation: Avila, A., M. Alarcón, S. Castillo, M. Escudero, J. García Orellana, P. Masqué, and X. Querol (2007), Variation of soluble and insoluble calcium in red rains related to dust sources and transport patterns from North Africa to northeastern Spain, *J. Geophys. Res.*, *112*, D05210, doi:10.1029/2006JD007153.

1. Introduction

[2] Arid regions in the Sahara and the Sahel provide large quantities of mineral dust which is distributed worldwide. The Saharan dust emissions have been estimated to be around 600–700 $\times$ 10^6 t yr^{-1} [*D'Almeida*, 1986; *Marticorena and Bergametti*, 1996]. The fate of this dust has been subject of a growing interest recently because of its effects on the human society (e.g., decrease in visibility and impact on air quality) and because of its direct or indirect effects on climate. Direct effects rise from the dust aerosol influence on the atmospheric radiative budget by absorbing/scattering radiation [*Li et al.*, 1996; *Tegen et al.*, 1996; *Sokolik et al.*, 1998] while indirect effects derive from its cloud nucleation potential when enriched in sulphate phases [*Levin et al.*, 1990; *Levin and Ganor*, 1996; *Rosenfeld and Lensky*, 1998]. There is also a potential feedback mechanism on climate due to the increased phytoplankton productivity as dust fertilizes the oceans [*Jickells et al.*, 2005]. Furthermore, because of its deposition of key mineral

[1]Centre de Recerca Ecològica i Aplicacions Forestals, Universitat Autònoma de Barcelona, Bellaterra, Spain.
[2]Departament de Física i Enginyeria Nuclear, Universitat Politècnica de Catalunya, Vilanova i La Geltrú Spain.
[3]Institut Jaume Almera, Consejo Superior de Investigaciones Científicas, Barcelona, Spain.
[4]Now at Institut Jaume Almera, Consejo Superior de Investigaciones Científicas, Barcelona, Spain.
[5]Institut de Ciència i Tecnologia Ambientals, Departament de Física, Universitat Autònoma de Barcelona, Bellaterra, Spain.

0148-0227/07/2006JD007153

nutrients, dust deposition is relevant in marine and terrestrial biogeochemical cycles [*Duce*, 1986; *Avila et al.*, 1998].

[3] Dust transport and distribution depends mainly on two factors: (1) the updraft of dust particles into the atmosphere and (2) their transport by large-scale atmospheric circulations to receptor areas. The atmospheric dust cycle ends with its deposition in dry or wet mode, a process that also affects the atmospheric dust distribution. The uprooting of dust in arid regions depends on terrain characteristics (such as soil composition, moisture content, vegetation cover and degree of disturbance) and on local atmospheric conditions, such as temperature and wind velocity [*Gillette*, 1979; *Marticorena et al.*, 1997]. Some studies have shown the occurrence of seasonal transport patterns and that specific source areas in Africa are active at different periods of the year. For example, seasonality is seen in Mali-Mauritania, western Sahara, Tunisia-Algeria, west Egypt; [*Prospero et al.*, 2002], but other source regions (e.g., the Bodele depression) are active during the whole year as shown by satellite imagery [*Moulin et al.*, 1997; *Prospero et al.*, 2002; *Barkan et al.*, 2004].

[4] An important fraction of the atmospheric dust load is carried in a westward direction to the tropical North Atlantic, reaching the eastern coasts of North America [*Prospero*, 1996; *Husar et al.*, 1997; *Perry et al.*, 1997], the Caribbean Sea [*Prospero and Carlson*, 1972; *Westphal et al.*, 1987] and South America [*Swap et al.*, 1992, 1996; *Formenti et al.*, 2001].This trans-Atlantic transport follows a seasonal regular pattern linked to the summer-winter movements of the position of the ITCZ with maximum arrival of dust to North America in summer and to South America early in the year [*Prospero and Carlson*, 1981; *Prospero*, 1996; *Moulin et al.*, 1997; *Perry et al.*, 1997].

[5] The Mediterranean Sea and its surrounding territories are also subject to very frequent outbreaks of mineral dust from Africa [*Löye-Pilot and Martin*, 1996; *Barkan et al.*, 2005]. The transport pathways here have been linked to the cyclonic activity over the Mediterranean and to the presence of high pressures over North Africa [*Moulin et al.*, 1997; *Rodríguez et al.*, 2001; *Barkan et al.*, 2005; *Escudero et al.*, 2005] and are, therefore, more irregular. Dust episodes in the Mediterranean basin tend to occur in a ''pulse-like mode,'' in intense but sporadic wet and dry deposition events. Most of the annual deposition load is accounted by a few episodes that may reach 60–80% of the total annual particle fallout [*Löye-Pilot et al.*, 1986; *Guerzoni et al.*, 1995].

[6] Wet African episodes in the Mediterranean are associated with depressions affecting the Mediterranean basin principally in late winter-spring and autumn [*Avila et al.*, 1997; *Escudero et al.*, 2005], while dry African intrusions mostly occur in summer when a persistent surface thermal low is formed over North Africa and the North African high moves to upper atmospheric levels. At altitude it injects the uplifted dust into a northward direction. Thus, contrary to maximum transport of dust over the Mediterranean in summer, wet dust deposition is maximum in spring and autumn in close correlation with the wet seasons in the basin [*Löye-Pilot et al.*, 1986; *Avila et al.*, 1997].

[7] Several studies have shown that African dust is made up of quartz (SiO_2), clay minerals (kaolinite, illite, smectite, palygorskite, chlorite), calcite ($CaCO_3$,) dolomite ($CaMgCO_3$), and feldspars [*Ganor*, 1991; *Molinaroli*, 1996; *Avila et al.*, 1997; *Guerzoni et al.*, 1997; *Caquineau et al.*, 1998], while iron oxides and calcium sulphate may also be present in minor proportions [*Glaccum and Prospero*, 1980; *Schütz*, 1989]. Although an homogenization of aerosols of African provenance by the mixing effect of winds and the resuspension processes has been proposed, many authors have found differences in mineralogical and chemical composition of African aerotransported dust depending on the lithology and the edaphic processes in the source regions [*Bergametti et al.*, 1989a, 1989b; *Ganor*, 1991; *Chiapello et al.*, 1997; *Caquineau et al.*, 1998, 2002]. Besides source area composition, further mineralogical and chemical differentiation at a far away receptor point may arise from selective transport processes occurring during the plume evolution: a downwind decrease in grain size and an enrichment of fine particles (clays) relative to coarse (quartz) has been reported [*Glaccum and Prospero*, 1980].

[8] Many studies have considered the chemical characteristics of the Saharan dusts transported to the Atlantic [*Swap et al.*, 1992; *Chiapello et al.*, 1997; *Stuut et al.*, 2005] or to the eastern [*Ganor et al.*, 1991; *Al Momani et al.*, 1997; *Koçak et al.*, 2004] and western Mediterranean [*Löye-Pilot et al.*, 1986; *Bergametti et al.*, 1989a; *Guerzoni et al.*, 1997; *Guieu et al.*, 2002]. Similar research for dust transported to eastern Spain includes the work of *Queralt-Mitjans et al.* [1993], *Avila et al.* [1997, 1998], *Querol et al.* [1998], and *Rodríguez et al.* [2001, 2002].

[9] In this paper we focus on the Ca composition (soluble and insoluble) of Saharan dust delivered by red rains at a rural site in northeastern Spain distinguished by provenance regions, and describe the dissolution processes occurring during transport. In the insoluble phase we have also analyzed the chemical composition for 17 elements for 30 filters and the ^{210}Pb concentrations in 23 samples. These comprise most major wet deposition events occurring at the site from 1983 to 2002 (except for two big events in 12 November 1984 and 24 April 1985 delivering together 20 g m^{-2} of dust where no elemental analysis could be performed). Such a long temporal series of dust collection is hardly found in the literature and encompasses all major situations of wet dust transport from Africa to the western Mediterranean area.

2. Material and Methods

[10] The sampling site was at 700 m a.s.l in a clearing of a dense holm oak forest (*Quercus ilex* L.) at La Castanya Biological Station (LC, 41°46′N, 2°21′E) in the Montseny mountains. The site is located in a rural area 40 km to the NNE from Barcelona, and lies at 25 km to the W of the Mediterranean Sea. The Montseny is a massif protected as a Natural Park; it is highly forested and the main human activities are in the sylvoagricultural and services sectors. Agricultural activities extend also in the surrounding areas. The lithology of Montseny is mostly composed of schists and granodiorites. The climate is humid Mediterranean, with a mean annual precipitation of 900 mm yr^{-1} in the period 1983–2000. Summer drought is present though attenuated by frequent orographic storms in August and September. Mean temperature at the site is 9°C.

Table 1. Collection Date of Red Rain Events and Descriptors for Meteorology and Source Area[a]

Collection Date	Rain Days	^{210}Pb Analysis	Elemental Analysis	Synoptic Pattern	Source Area	Precipitation, L m^{-2}	Dust Deposition, mg m^{-2}
4 Nov 1987	28 and 29 Oct 1987	yes	yes	AD to NAD	W	42.5	1013.3
5 Dec 1987	3–5 Dec 1987	yes	yes	AD	W	70.9	3989.2
9 May 1988	6–8 May 1988	yes	yes	NAD	E	5.3	1402.1
27 Jun 1988	23–26 Jun 1988	yes	yes	AD	W	14.3	975.0
15 Oct 1990	9–15 Oct 1990	yes	yes	NAD to AD	W	105.0	776.0
23 Oct 1990	22 Oct 1990	yes	yes	AD	W	26	621.2
11 Mar 1991	5 and 6 Mar 1991		yes	AD to NAD	E	26.9	2958.0
28 Mar 1991	24 and 25 Mar 1991	yes	yes	NAD	E	169.0	19435.0
17 Apr 1991	17 Apr 1991		yes	NAD	E	0.9	215.0
16 Oct 1991	9–11 Oct 1991		yes	AD	E	15.4	6730.8
11 Mar 1992	4–6 Mar 1992	yes	yes	NAD	CA	22.6	2739.0
22 Jan 1996	21 and 22 Jan 1996	yes	yes	AD	W	30.7	218.0
29 Jan 1996	22–24 Jan 1996	yes	yes	AD	W	91.7	518.1
21 Nov 1996	12–17 Nov 1996	yes	yes	AD	W-n	256	6440.0
27 Jan 1997	24 and 25 Jan 1997	yes	yes	NAD	mix	14.5	623.0
20 Aug 1997	10 and 11 Aug 1997	yes	yes	NAH-H	W	59.9	421.0
3 May 1999	28 and 29 Apr and 2 and 3 May 1999		yes	NAD	E	5.3	1000.1
10 May 1999	3, 4, 6, and 7 May 1999	yes	yes	NAD to AD	W-n	10.4	102.3
17 May 1999	13, 16, and 17 May 1999	yes	yes	NAD	E	24.6	280.4
25 May 1999	17–19 May 1999	yes	yes	NAD	E	24.2	248.7
31 May 1999	26 May 1999		yes	AD	mix	0.5	291.0
7 Jun 1999	5 and 6 Jun 1999		yes	NAH-H	E	1.0	68.2
14 Jun 1999	9, 12, and 13 Jun 99		yes	NAD	W-n	19.8	1001.0
17 Aug 1999	27 and 28 Jul 1999	yes	yes	AD	W-n	59.7	816.6
15 Nov 1999	11 and 12 Nov 1999	yes	yes	NAD	W	80.3	5553.0
27 Mar 2000	25–27 Mar 2000	yes	yes	NAH-S	W	4.8	212.0
17 May 2000	10–12 May 2000	yes	yes	AD	W	23.9	338.0
23 Aug 2000	13 Aug 2000	yes	yes	NAH-H	W	41.1	238.1
7 Sep 2000	30 Aug and 4 Sep 2000	yes	yes	NAH-H	E	21.0	75.0
3 Apr 2002	2 and 3 Apr 2002	yes	yes	NAD	W	45.0	50.5

[a]Dust deposition (in mg m^{-2}) is also given. AD, Atlantic depression; NAD, North African depression; NAH-H, North African high pressure at height; NAH-S, North African high pressure at surface, from *Escudero et al.* [2005]; W, western; E, eastern; W-n, northwestern provenances with respect to 0° Greenwich; CA, central Algeria.

[11] At this site we collected weekly rainfall samples from July 1983 to December 2003, with a break comprising all year 2001. Precipitation for analysis was collected in 4 open bulk deposition collectors from January 1983 to May 1993 and with 2 collectors thereafter. Reduction of replication did not affect the analytical results [*Avila*, 1996]. Because the collectors were continuously open to the atmosphere, the samples strictly refer to bulk deposition. At Montseny, dry deposition of sedimented particles has been found not to modify to a great extent the chemical signal of wet precipitation [*Avila and Alarcón*, 1999]. For the particle matter, collection during non-red rain events was negligible compared to the weights collected with African rains (mean of 39.5 mg/filter for red rains, n = 84 filters, compared to <0.1 mg/filter for non-red rains). The collectors were placed 1.5 m above the ground and consisted of a 19-cm diameter-polyethylene funnel connected by tygon tubing to a 10-L polyethylene bottle with a clean nylon sieve in the neck of the funnel to prevent inclusion of insects and vegetal debris. In each weekly visit, collectors were retrieved and replaced by laboratory-cleaned ones. Cleaning procedures included a wash of all disassembled parts with laboratory cleaning detergent, followed by a profuse rinse with deionized distilled water. Collecting bottles were rinsed with diluted HCl to minimize adsorption on the inner bottle walls, followed by a through rinse with deionized distilled water. In 2002, samples were obtained from a dry/wet deposition collector (Andersen) installed at La Castanya station.

[12] Because the sampling extended for such a long period, care was taken that the protocols were strictly followed in field and laboratory tasks. The materials for the collectors (funnels, tubing and bottles) were always of the same type (polyethylene for funnels and bottles, tygon for tubing) and were replaced by new material when visual observation indicated the onset of deterioration, about once every two years.

[13] African dust events were clearly recognized because of the brown-reddish drop marks on white funnel walls and also by some residue being often accumulated in the tygon loops. This material was also carefully collected and weighted, and it was added to the weights obtained by filtering known rain volumes, to produce the final total dust deposition. We selected for analysis the major events in the period 1983–2002. This produced a batch of 30 filters for the elemental analysis and 23 for ^{210}Pb analysis (Table 1). These major events comprised 73% of the wet dust fall collected in the period (excluding events on 12 November 1984 and 24 April 1985 accounting together 20 g m^{-2} of dust, this percentage rises to 93%).

[14] Upon sampling, rainwater was taken to the CREAF laboratory where conductivity, pH and alkalinity were measured within 24–48 hours in unfiltered samples and samples were filtered through 0.45 μm pore size Millipore filters. The soluble samples were deep frozen (−20°C) for later analyses of major ions, and filters were dried at 100°C and reweighted to determine the deposition of insoluble material. Filters were stored in Millipore capsules for later

analysis. The filtered rain samples were analyzed for major cations by Atomic Absorption and Emission Spectroscopy, anions by Ion Chromatography, and ammonium by FIA colorimetry [*Avila*, 1996].

[15] To determine metal concentrations in the filters, we used the procedure developed at the laboratory of Institute Jaume Almera-CSIC [*Querol et al.*, 2001]. A half of each filter was digested in closed PFA reactors with HNO_3:$HClO_4$:HF at 90°C. Subsequently, the acidic solution was cooled and dried on a hot plate at 200°C. The dry residue was redissolved in 2 mL of HNO_3 and subsequently made to volume of 25 mL. The contents of major elements were determined by means of ICP-AES (Inductively Coupled Plasma Atomic Emission Spectometry) at the Institute Jaume Almera-CSIC. Blank values corresponding to blank Millipore filters (very low values with respect to the measured samples) were substracted from measured concentrations. Certified reference materials (1633b, and reference samples SO-1-dust, MAG-1-marine mud) were run throughout the analyses. The measured values were within 10% of the certified data. Replicate analysis for three filter pairs produced highly reproducibility (within 15% for all elements, except for Zn and Cu with coefficient of variation between replicates varying between 15 and 30%).

[16] ^{210}Pb activities were determined by measuring its daughter nuclide ^{210}Po in radioactive equilibrium following the methodology described by *Sanchez-Cabeza et al.* [1998]. Briefly, aliquots digested for the ICP-AES analysis were spiked with 1 mL addition of ^{209}Po as internal tracer. Polonium isotopes were plated onto high pure silver discs and counted with α-spectrometers equipped with low background silicon surface barrier (SSB) detectors (EG&G Ortec) at the Physics Department of the Universitat Autònoma de Barcelona.

[17] Back trajectories were obtained with the NOAA ARL HYSPLIT4 model [*Draxler and Rolph*, 2003] (http://www.arl.noaa.gov/ready/hysplit4). HYSPLIT4 was used with reanalysis meteorological data from the NCEP archive of NOAA's Climate Diagnostics Center (http://www.cdc.noaa.gov/cdc/data.ncep.reanalysis.html). Meteorological synoptic maps were obtained at the HYSPLIT address for all rainy days for the sampled events from 1996 onward; for the previous years, meteorological maps were consulted from the Europaïscher Wetterbericht, at the Physics Department of the Universitat de Barcelona. Additionally, in the pertinent cases, the synoptic situation for the previous dry days was also analyzed to account for dry plume transport before the occurrence of rain. Satellite images (Seawifs project_NASA [*McClain et al.*, 1998]), TOMS [*Herman et al.*, 1997] and dust models (SKIRON [*Kallos et al.*, 1997], http://forecast.uoa.gr/), DREAM [*Nickovic et al.*, 2001] (http://bscct01.bsc.es/DREAM/) and NAAPs (http://www.nrlmry.navy.mil/aerosol/) were also consulted, if available, to determine source areas. However, because of the length of the series, this type of material was not available for most of the events.

3. Results

[18] The weekly samples analyzed here are listed in Table 1, where the days of the rain are also shown. Mean rain duration was 2.8 days per event, ranging from single rain days to events lasting up to the whole week. The longest red-rain periods occurred in autumn.

3.1. Source Regions and Meteorological Setting

[19] The meteorological setting, the back trajectories corresponding to the rain days (at 12.00 h UTC) responsible of the African transport and satellite images (from 1999 on) were used to indicate the provenance regions, which are also listed in Table 1. Diagnostic back trajectories were usually taken at 1500 m but in some cases other levels have been also used.

[20] In a previous work, the meteorological scenarios responsible for the transport of African suspended particulate matter and wet deposition to northeastern Spain have been described [*Escudero et al.*, 2005]. Four scenarios emerged, two mostly associated to wet and two for dry transport. Wet African events in northeastern Spain are mostly produced by two major meteorological synoptic situations involving the presence of depressions associated to frontal situations. One is produced by an Atlantic depression (named AD), with a relatively deep low pressure situated west or southwest of Portugal and often associated with a ridge over the central Mediterranean Sea. This situation produces a southerly synoptic flow highly coherent at all altitude levels. In our analyzed samples 9 events (or 30% of the record) corresponded to this meteorological pattern (Table 1). Source areas under these conditions are usually from the west of the Sahara. A second frontal type is defined by a depression over North Africa (thereafter named NAD), where a ground level deep low is found over Morocco, Algeria, Tunisia, or even over the western Mediterranean. This situation favors the transport of African air masses toward the Iberian Peninsula across the Mediterranean. In this case the air mass transport is mostly confined to the lower layers. The dust sources usually are from the east (defined here as east of Greenwich), and although they are mostly situated in northern latitudes (northern Algeria and Tunisia), they also can proceed from central Algeria; in our record, they comprised 11 (37%) of the samples (Table 1). This NAD situation has been described to be the main transport mechanism toward Italy and central Europe [*Borbély-Kiss et al.*, 2004; *Barkan et al.*, 2005]. The Iberian Peninsula, situated at the westernmost extreme of south Europe, is subject to an Atlantic driven transport besides the central Mediterranean transport. At our site, the African transport linked to the AD scenario occurs mainly in winter, peaking in March, while that from the NAD is more frequent in May and November [*Escudero et al.*, 2005]. The mean synoptic situation for the eastern and western events in our study (geopotential height for 850 and 700 hPa calculated from the NOAA daily data for the days in each event) is given in Figure 1.

[21] Dry transport was linked to high-pressure systems installed over North Africa. Although these situations produced dry outbreaks over the Iberian Peninsula, in some cases rain was also present, as described next. In one of these types (named NAH-S), the high-pressure system was located at surface level and produced dust fluxes into the North Atlantic in an arch-like pattern. These were very frequent at the end of winter (February and March) and reached the Iberian Peninsula through the northwestern corner. In our wet dust samples, only one event corre-

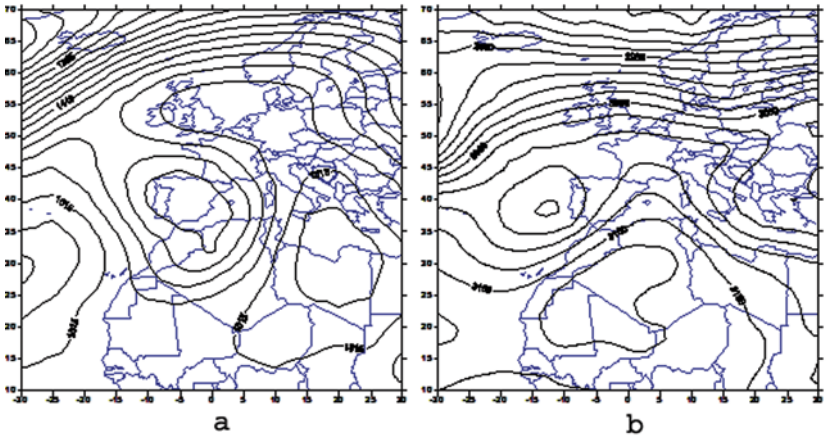

Figure 1. (a) NAD synoptic situation; mean maps of geopotential height (m) at 850 hPa. (b) AD synoptic situation; mean maps of geopotential height at 700 hPa.

sponded to this situation (27 March 2000) when an eastward Atlantic front probably impacted on the dust plume as it was traveling over the Atlantic. The other scenario for dry suspended matter transport was typical for summer (NAH-H) when the intense heating over the Sahara induces the development of the North African thermal low and the uplift of dust up to around 5000 m. Then, the dust is transported to the Iberian Peninsula by the western branch of the high situated at upper levels. Four of our analyzed rain events corresponded to this scenario (Table 1), usually occurring in summer when orographic convective rains at the receptor site scavenge the previously transported dust. Under this meteorological setting, the dust source region as traced by back trajectories, can either be from eastern or western provenances.

[22] Because of the weekly length of sampling in some events the synoptic situation evolved from one to another type, mostly from AD to NAD or vice versa (Table 1). In these cases the source area has been identified by taking into account the predominance of the area hit by the back trajectories.

[23] Some authors [*Prospero et al.*, 2002; *Stuut et al.*, 2005; *Escudero et al.*, 2006] have cautioned against the use of back trajectories to identify source areas. Back trajectories do not necessarily show the region where the dust has been uplifted because air masses can pick dust arisen from different source areas as they cross with their path. It has been suggested that satellite images or models may be needed to more precisely point to the precise source areas. Such a situation (satellite images showing a particular dust flux but back trajectories not representing it) particularly applied to events on 17 and 25 May and 7 June 1999. In these cases, provenances have been decided upon satellite observation. When we lacked satellite images we have made use of back trajectories, but because of their imprecise diagnostic nature, we have made a broad distinction between western and eastern air mass fluxes pragmatically differentiated with respect to 0° Greenwich (Figure 2). In the western flux, the analysis of data has asked for a further division to differentiate a northern (W-n) and a southern pathway from west Sahara (W). For the eastern flux (E), 5-day back trajectories hardly went further south than 30°N (Figure 2). In Table 2 we show the average length of the trajectories from western and eastern pathways for the 500, 1500 and 2500 m asl levels. It can be seen that eastern trajectories are shorter than western ones at all altitudes, with maximum difference (1634 km) at the 1500 m level.

[24] It has also to be noticed that most of the contributing sources to our site, either coming from the west or the east, are mostly from above the 25° latitude, as also described for Corsica [*Bergametti et al.*, 1989a]. This implies that only the northern Sahara is involved in transport to the northwestern Iberian Peninsula, with some exceptions such as the event on 27 March 2000 (not shown) when a dust plume

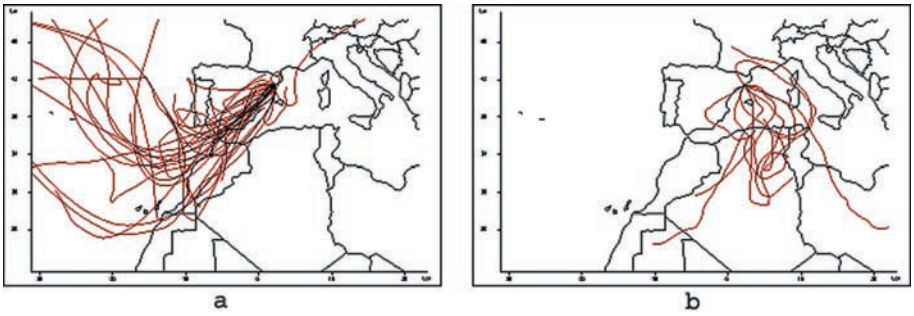

Figure 2. Back trajectories from (a) western and (b) eastern provenances at 1500 m asl. For a sampled episode, several days of African flux are represented according to Table 1.

Table 2. Mean Length of 5-Day Back Trajectories at Three Altitude Levels (500, 1500, and 1500 m asl) Arriving at Montseny (41°46′N, 2°21′E), With Provenances Classified as Coming From West or East With Respect to 0° Greenwich[a]

Length, km	500 m	1500 m	2500 m
Western	3451	3995	4605
n =	15	18	24
Eastern	2559	2321	3231
n =	7	6	3

[a]The number of observations is different because not all back fluxes came from the east-west direction but came from other quadrant provenances.

moved over the Atlantic in an arch-like pathway probably coming from more southern positions and the event on 11 March 1992, from southern and central Algeria.

3.2. Dust Composition

[25] The amount of insoluble material in red rains sampled at Montseny was highly variable: from a few mgL^{-1} to a maximum 437 mgL^{-1}. The corresponding precipitation was also highly variable (<1 Lm^{-2} to 256 Lm^{-2}, Table 1). The particulate material deposition fluxes varied in accordance, from less than 1 mg m^{-2} to a maximum of 19.4 g m^{-2}. At Montseny, the total measured insoluble material deposited with red rains from 1983 to 2000 was 82.0 g m^{-2}, which gives an annual average of 4.6 g m^{-2}. This is a moderate deposition flux, compared with recorded values in the central Mediterranean (12–14 g m^{-2} in Corsica [*Löye-Pilot et al.*, 1986; *Bergametti et al.*, 1989a]) and the eastern Mediterranean coast (20–40 g m^{-2} in Israel [*Ganor and Mamane*, 1982]).

[26] The African dust reaching Montseny with red rains is made up of quartz, clay minerals (illite, smectite, kaolinite and palygorskite), feldspars and calcite. Previous work at this site has shown that smectite and kaolinite were higher in dusts from the most distant source areas, while quartz and calcite where higher in events from Morocco [*Avila et al.*, 1997].

[27] To interpret the dust chemical data we applied a PCA to the elemental analysis of the 30 insoluble dust samples, considering the concentrations of Al_2O_3, CaO, Fe_2O_3, K_2O, MgO, Na_2O, P_2O_5, TiO_2, Ba, Cr, Cu, Mn, Ni, Pb, S, Sr, V, Zn, ^{210}Pb and the dust amount. The results are shown in Table 3, where only the variables with factor loads higher than 0.7 are shown. Three factors accounted for 69.4% of the variance. A strong opposition in crustal-derived elements was found in factor 1: calcite and dolomite-derived elements (Ca, Mg and Sr) were opposed to clay silicates-derived elements (Al, V) and Fe. For V, while in atmospheric aerosols it is mainly derived from fossil fuel emissions, V(III) is also present in clay minerals substituting Al(III). Factor 2 presented high loadings (in the negative section) of S, Zn, Cu and Ni. The enrichment in these trace metals and S would indicate the influence of anthropogenic derived contamination. Factor three only included Mn, with only 11.5% of the variance explained.

Table 3. Varimax Rotated Factor Loadings Obtained With a Principal Component Analysis for the Chemical Analysis of the Insoluble Residue of 30 Dust Samples From Red Rains Arriving at Montseny[a]

Variable	Factor 1	Factor 2	Factor 3
Al_2O_3	−0.97		
Fe_2O_3	−0.88		
V	−0.79		
CaO	0.97		
Sr	0.93		
S		−0.91	
Zn		−0.92	
Cu		−0.89	
Ni		−0.78	
Mn			0.75
Variance	34.3	23.6	11.5

[a]Only factors >0.7 are shown.

[28] In Figure 3, we have plotted the scores of the samples for the two main factors. In this graph, three groups can be distinguished. The samples from eastern sources (E, squares) are situated at the positive side of factor 1, indicating higher concentrations of the "carbonated lithology" defined by high Ca, Mg, Sr concentrations. On the contrary, samples from the western Sahara (W, solid circles and W-n, open circles) lie in the "silicate lithology" side, defined by Al, Fe, K and V.

[29] It can be seen that some of the samples from the western provenances tended to score to the negative side of factor 2, indicating a contribution of anthropogenic-derived elements. These samples corresponded to trajectories arriving from Morocco, the northern part of the western provenance (W-n, in Table 1). Therefore, to account for these chemical differences, we have split the western group into 2 subgroups, one including the 4 Moroccan trajectories (W-n, open circles in Figure 3), and the other with the rest of the western samples (n = 13). In Table 4 we present the mean crustal chemical composition by provenance groups.

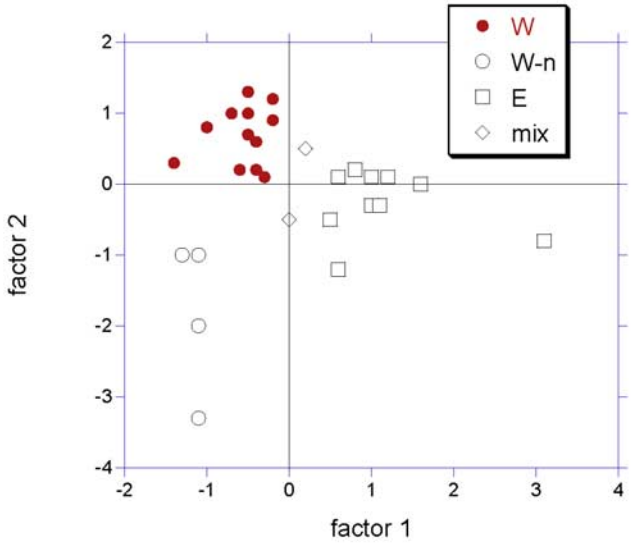

Figure 3. Principal component analysis applied to the elemental composition of the insoluble dust delivered by red rains at Montseny: scores of the individual samples, distinguished by provenance region. Western (W) is indicated by solid circles, western-north (W-n) is indicated by open circles, eastern provenance (E) is indicated by open squares, and mixed events are indicated by diamonds.

Table 4. Mean and Standard Error of Crustal Elements in the Insoluble Residue of African Dust at Montseny by Provenance Groups[a]

	Silicate-Derived					Carbonate-Derived				
Provenance	Al, %	Fe, %	K, %	P, %	V, ppm	Ca, %	Mg, %	Sr, ppm	Na, %	Ti, %
Western										
Mean	10.3(a)	5.73(a)	3.07(a)	0.24(b)	137(b)	1.57(a)	2.13(a)	146(a)	0.30	0.58
Standard error	0.08	0.04	0.07	0.03	3.88	0.17	0.08	3.89	0.07	0.02
Western-north										
Mean	10.0(a)	5.88(a)	3.20(a)	0.41(a)	155(a)	1.78(a)	1.84(a)	167(a)	0.77	0.70
Standard error	0.21	0.24	0.14	0.06	10.3	0.34	0.16	11.3	0.19	0.03
Eastern										
Mean	8.25(b)	4.73(b)	2.67(b)	0.15(c)	110(c)	7.41(b)	2.41(b)	242(b)	0.54	0.55
Standard error	0.19	0.12	0.03	0.03	10.4	0.51	0.17	32.0	0.03	0.01

[a]Significant differences by ANOVA comparison between groups ($p < 0.05$) are indicated by letters a, b, and c in parentheses. Two samples of mixed origin (27 January 1997 and 31 May 1999) were excluded from the analysis. For western provenances n = 13, western-north n = 4, and eastern n = 10.

It can be seen the lack of significant differences in crustal elements between the two western groups and their significant differences to the eastern events. Higher concentrations of Al, Fe, K, P and V were found in western samples, while the eastern ones were significantly richer in Ca, Sr, and Mg (Table 4). This opposite behavior is best seen in the highly significant relationship ($r^2 = 0.98$; n = 30) of CaO versus Al_2O_3 (Figure 4). In this graph, all western samples concentrated to the right, with the highest Al and lowest Ca insoluble concentrations. Eastern samples extended over a wider range of values, but they were clearly differentiated from the western ones. In between the two groups lay two samples of mixed origin (27 January 1997 and 31 May 1999).

[30] The two western groups could not be distinguished by the crustal elements but they were distinctly different when looking at the trace metal content. Dust from Morocco had significantly higher concentrations for S, Ni, Cu, and Zn than the other provenances (Table 5). When comparing their enrichment factors (enrichment factor defined as $Ef(x) = (X/Al)_{dust}/(X/Al)_{crust}$, with (X/Al) with crustal values taken from *Taylor and McLennan* [1985]), although our highest values were much lower than those reported for African aerosols collected in the northern border of the Mediterranean [*Chester et al.*, 1993; *Guieu et al.*, 1997], the Moroccan group showed higher values (except for Cr) than the other provenances (Table 5). On the other hand, ^{210}Pb was significantly higher in western provenances compared to those from Morocco and from eastern trajectories.

4. Discussion

[31] Higher concentrations for the anthropogenic-derived elements in the Moroccan provenances are not unexpected because of their more probable interaction with atmospheric fluxes from the European continent. As an example, the event collected on 14 June 1999 was produced by rain in the previous day. Back trajectories in 13 June indicated that the lower fluxes originated from Europe and the Iberian Peninsula, while at higher altitudes, the flux proceeded from Africa (Figure 5). Such combined European and African fluxes may explain the high sulphate values often encountered in red rains [*Avila and Rodà*, 1991]. This deserves further attention but is beyond the scope of this paper.

[32] We will focus here on the variations shown by the soluble-insoluble Ca depending on the provenance distinction. When considering the insoluble phase, eastern samples were enriched in calcite-derived elements (Ca, Mg and Sr) and depleted in silicate-derived elements (Al, K, V, Fe). As a consequence, the element ratios were also distinctly different (Table 6) with X/Ca (X = Al, Fe, Mg, K, P) ratios being significantly higher in western provenances. However, when we consider bulk Ca (the soluble plus insoluble fractions of Ca) normalized versus the other elements, the above differences disappear (Table 6). This has several implications: First, bulk Ca content is not an appropriate tracer to distinguish for source areas as might be insoluble Ca. However, at the emission point when dust is uplifted, bulk Ca is the relevant variable to consider because solubilization has not yet taken place. The lack of differences in bulk Ca between provenances point to a similar lithology between both areas.

[33] In fact, both the Tunisia area and most of the western Sahara lie upon carbonated lithology. In the occidental Sahara, the Coastal Basin (also referred as El AAiun-Tarfaya Basin) is composed of Mesozoic and Cenozoic carbonatic sediments, dolomites and marls. By contrast, Precambrian and Paleozoic massifs with low carbonate content cover more southern parts comprising Chad, Sudan, Mali, Mauritania and the coastal regions of Ghana, Cote d'Ivore, Guinea. (Figure 6 [*Moreno et al.*, 2006]). In agreement, relatively high calcite (and consequently Ca) contents have been reported for the dust of west Sahara

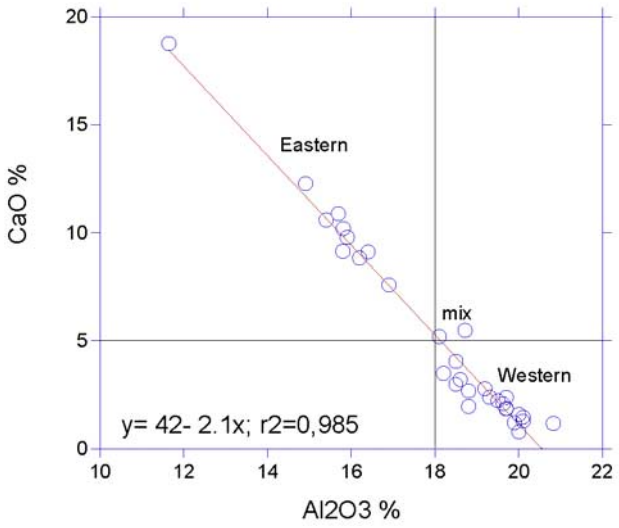

Figure 4. Scattergram of CaO versus Al_2O_3, distinguished by provenance region.

Table 5. Mean and Standard Error of Anthropogenic Elements in the Insoluble Phase of African Dust at Montseny by Provenance Groups[a]

	S, %	Cu, ppm	Ni, ppm	Zn, ppm	Pb, ppm	Ba, ppm	Mn, ppm	Cr, ppm	^{210}Pb, kBq kg^{-1}
Western, n = 13									
Mean	1.25(a)	113(a)	86.0(a)	939(a)	231	587	816	196	5.33(a)
Standard error	0.04	22.9	12.0	178	49.5	18.2	19.4	49.5	0.71
EF	4.1	3.5	3.4	10.3	9.0	0.8	1.1	4.4	
Western-north, n = 4									
Mean	4.00(b)	644(b)	372(b)	6394(b)	403	767	739	93.5	2.90
Standard error	0.17	266	83.3	103	10.3	112	41.4	31.2	1.29
EF	13.3	21.0	15.0	72.6	16.2	1.1	1.0	2.2	
Tunisia, n = 10									
Mean	1.07(a)	112(a)	110(a)	1011(a)	147	633	743	235	1.32(b)
Standard error	0.03	75.2	36.2	641	11.8	69.0	29.3	103	0.29
EF	4.4	4.4	5.4	13.9	7.2	1.1	1.2	6.6	

[a]Significant differences by ANOVA comparison between groups ($p < 0.05$) are indicated by letters a, b, and c in parentheses. Two samples of mixed origin (27 January 1997 and 31 May 1999) were excluded from the analysis. Enrichment factors (EF) with respect to *Taylor and McLennan* [1985] values are also given for each provenance group.

compared with that from the Bodele depression lying in a more southern position [*Paquet et al.*, 1984; *Chiapello et al.*, 1997].

[34] Many studies have aimed at fingerprinting the chemical characteristics of source areas in North Africa. In Table 7 we have compiled some elemental ratios from the bibliography and compare them to our results. The comparison has been organized as to put together data from broadly similar areas, distinguishing a western and eastern provenance with respect to 0° Greenwich. Source areas have been usually recognized by the authors through back trajectory analysis, satellite imagery and meteorological flow patterns so we can identify origin areas similar to those defined in this work.

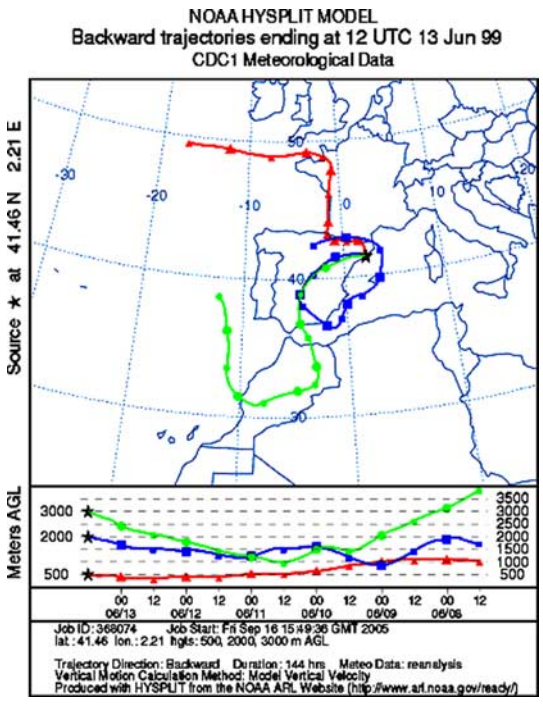

Figure 5. HYSPLIT back trajectories (at the 500, 2000, and 3000 m asl levels) for the red rain event on 13 June 1999 collected on 14 June 1999 at Montseny (northeastern Spain).

[35] Because of the mentioned ratio differences whether considering insoluble or bulk Ca, we present in Table 7 our element ratios both to insoluble Ca and to bulk Ca. The ratios to bulk Ca would approach the situation at the origin, while the ratios to insoluble Ca would represent the disappearance of Ca from the insoluble residue due to dissolution and would indicate the interaction of the aerosols with a dissolving wet phase during transport. It can bee seen that the values from the literature are mostly comprised within our range, in accordance with the fact that they come mostly from aerosol studies with little dissolution because of a scarce wet interaction with the mineral phase. However, when looking in more detail, we observe that for the eastern provenances, our ratios Fe/Ca and K/Ca are lower than the values from the literature, both for the insoluble and the total Ca. On the other hand, Fe/Al ratios of samples collected at Montseny were equal for both provenances (0.56) and within the range of values given in the literature for both source regions (Table 7).

[36] Because of the ratio differences whether considering insoluble or bulk Ca, we calculated the Ca mass balance, for soluble Ca by multiplying rain Ca concentrations (sea salt corrected) by the rain amount, and for insoluble Ca, by multiplying the % Ca by the particle matter deposition for the coincident events. Results (Table 8) indicate that the major Ca differences between provenances are in the insoluble-soluble partitioning, with soluble Ca accounting for 91% of total Ca in western samples and only 31% in the eastern ones.

4.1. Carbonate Dissolution

[37] To investigate whether differences in the soluble fraction arose from a differential dissolution rate of carbo-

Table 6. Element Ratios in the Insoluble Phase by Provenance at Montseny[a]

	Ca/Al	Fe/Ca	K/Ca	Ti/Ca	Mg/Ca	P/Ca	Fe/Al	Ti/Fe
Western								
Mean	0.14	3.90	2.01	0.38	1.45	0.11	0.56	0.10
Standard deviation	0.07	0.12	1.08	0.26	0.51	0.16	0.01	0.01
Eastern								
Mean	1.31	0.43	0.26	0.05	0.31	0.01	0.56	0.12
Standard deviation	0.28	0.48	0.08	0.02	0.06	0.01	0.04	0.01

[a]For western n = 13, and for eastern provenances n = 10.

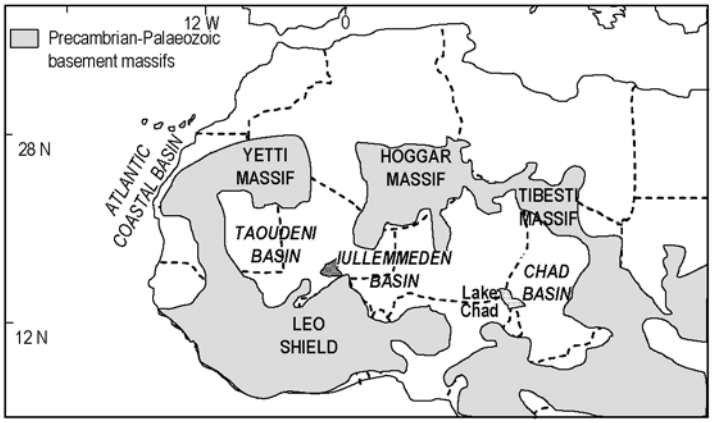

Figure 6. Map of northern Africa showing the distribution of large Precambrian and Paleozoic basements with relatively low limestone sequences. Open areas are mostly carbonated lithologies. Reprinted from *Moreno et al.* [2006] with permission from Elsevier.

nates in rain depending on the origins, we have used the equilibrium equations of the carbonate dissolution [*Stumm and Morgan*, 1981]. We will examine the hypothesis that the lower insoluble CaO, MgO, and Sr content in western Africa fluxes was due to higher dissolution of calcareous particulates in rainwater from this provenance. If this was the case, we would expect lower CaO and MgO in the solid residue, which we observe (Table 4) and higher concentrations of the soluble products of carbonate dissolution in rain (specifically, higher Ca^{+2} and HCO_3^- ions) in western rainwater samples compared to the eastern ones. Therefore the relationship between the solid phase and the soluble products should be inverse and distinct for the two groups of samples. In Figure 7, we present the scattergrams of the soluble Ca^{+2} and HCO_3^- concentrations related to the solid phase CaO concentrations. It can bee seen that the dusts from the eastern provenance are distinguished by a higher solid phase content but are not different from western samples in the soluble concentrations: all the samples lie in the range between 10 and 1000 μeq L^{-1} Ca^{+2} or HCO_3^- soluble concentrations (in logarithmic scale in Figure 7), and in any case, the Ca^{+2} and HCO_3^- arithmetic mean is lower in western samples, contrary to the initial assumption.

[38] If calcite was dissolving in rainwater, the equation defined by the solubility equilibrium of calcite should govern the presence of the dissolved species Ca^{+2}, HCO_3^- and H^+. Assuming that all HCO_3^- present in a solution comes from $CaCO_3$, the relationship between pH and $\log(HCO_3^-)$ is defined by the expression (in molar terms [*Stumm and Morgan*, 1981]):

$$\log\left(HCO_3^-\right) = 0.5(\log 2 - p^*K_s - pH), \quad (1)$$

where $p^*K_s = -\log(K_{cal}/K_2)$,
Alternatively, Ca^{+2} concentrations can be expressed as a function of HCO_3^-:

$$\log\left(Ca^{+2}\right) = pK_{cal}\, pK_1\, pK_H\, pCO_2/pK_2 \log\left(HCO_3^-\right), \quad (2)$$

where K_{cal} is the solubility product of calcite ($10^{-8.35}$), K_H ($10^{-1.47}$) is the equilibrium constant of the CO_2 solubility in water and K_1 and K_2 are the first and second constant of the carbonic acid system ($10^{-6.35}$, $10^{-10.33}$, respectively, all constants given at 25°C). pCO_2 is the CO_2 concentration, here taken as the atmospheric ($10^{-3.5}$); prefix p indicates that the logarithm of the equilibrium constants is changed in sign.

[39] In Figure 8 we plot the soluble concentrations (in logarithms) of HCO_3^- versus pH in the events for which we have analyzed the dust residue, classifying the samples by provenance: we do not observe differences between either provenance and the relationship between HCO_3^- and pH in the samples seems to be governed by the equilibrium of CO_2 dissolution and the carbonic acid system defined by [*Stumm and Morgan*, 1981]:

$$\log\left(HCO_3^-\right) = pH - pK_1 - pK_H + pCO_2. \quad (3)$$

[40] The distribution of the points goes in parallel for the two subsets of samples and most of them are included in two enclosing positive lines. These lines are defined by the above relationship considering atmospheric pCO_2 ($pCO_2 = 10^{-3.5}$; line b) and 10 times atmospheric pCO_2 ($pCO2 = 10^{-2.5}$; line c). The upper boundary line, with a negative slope (line a) is defined by equation (1), and represents the boundary where HCO_3^- concentrations governed by calcite dissolution should lie. The fact that the points are far apart from the calcite equilibrium boundary and that they do not show any correlation with this line indicates that the soluble phase is far from calcite saturation. On the other hand, the parallel relationship of the points distribution with the lines defined by the carbonic acid system would indicate that the dissolution of CO_2 is the primary factor governing rainwater HCO_3^-, pH and soluble Ca^{2+} in dust laden rainfall and that it equally affects eastern and western events.

4.2. Fractionation and Dissolution During Transport

[41] On the other hand, another possibility to explain the differences in the soluble-insoluble Ca fractions is related to the occurrence of selective processes during transport. Longer transport of dust would favor the deposition of the coarsest particles, resulting in an enrichment of the finer

Table 7. Elemental Ratios From Literature Studies of North African Dust Compared to Those Obtained at Montseny[a]

	Si/Al	Fe/Al	Al/Ca	Fe/Ca	K/Ca	Mg/Ca	P/Ca	Ti/Fe	Ti/Ca	Type of Sample	Date of Sampling	Sampling Site
Western (20–35°N, 5–20°W)												
Bergametti et al. [1989b]	2.7–2.8	1.0–1.2								aerosols	18–31 Jul 1985	Fuerteventura (Canary Islands)
Coudé-Gaussen et al. [1987]			3.45				0.02		0.02	aerosols	18 Apr 1984	Fuerteventura (Canary Islands)
Viana et al. [2002]			1.11	0.58	0.32	0.35	0.023			aerosols	Feb 2001 (two events)	Tenerife (Canary Islands)
Bergametti et al. [1989a]	2.7–2.9	0.7–0.9	1.20	0.99						aerosols	Feb 1985 to Apr 1986	Capo Cavallo (Corsica)
Bonelli et al. [1996]	2.72	0.67	1.30	0.87	0.35				0.09	aerosols	24 Mar 1991	Stelvio (N-Italy)
Chiapello et al. [1997]	2.32	1.5	1.66	0.90	0.43					aerosols (sector 3)	1991–1994 (winter)	Sal Island
Stuut et al. [2005]		0.42						1.30		aerosols (samples 1 to 4)	Feb–Mar 1991	Cruise west African coast
Gatz and Prospero [1980]	2.0		2.50	2.0						aerosols	29 Jul 1979	Illinois (EUA)
Blanco et al. [2003]	2.44		2.70	0.60	0.73					rain dust residue	Apr–Jun 2002	Lecce (S.Italy)
This work (bulk Ca)		0.56	0.65	0.35	0.20	0.14	0.01	0.10	0.04	insoluble + soluble in red rains	1983–2002	Montseny (NE Spain)
This work (insoluble Ca)		0.56	6.67	3.90	2.10	1.45	0.11	0.10	0.38	insoluble in red rains	1983–2002	Montseny (NE Spain)
Eastern (25–35°N, 0–15°E)												
Bergametti et al. [1989a]	2.2	0.52								aerosols	Feb 1985 to Apr 1986	Capo Cavallo (Corsica)
Blanco et al. [2003]	2.10	0.23	4.35	0.98	1.34					dust residue in rains	Apr–Jun 2002	Lecce (S. Italy)
Bonelli et al. [1996]	2.12	0.55	1.96	1.08	0.42				0.11	aerosols	24 Mar 1991	Stelvio (N. Italy)
Borbély-Kiss et al. [2004]		0.8–1.7	0.7–0.9	0.7–1.2				0.1–0.07	0.07–0.09	aerosols	1991–2000	Debrecen (Hungary)
This work (bulk Ca)		0.56	0.53	0.30	0.18	0.22	0.01	0.12	0.04	insoluble + soluble in red rains	1983–2002	Montseny (NE Spain)
This work (insoluble Ca)		0.56	0.76	0.45	0.26	0.31	0.01	0.12	0.05	insoluble in red rains	1983–2002	Montseny (NE Spain)
Soils in central Sahara [*Guieu and Thomas*, 1996]	3.92	0.61	3.57	2.19	0.86		0.17		0.36	soil (fraction <50 μm)		South Algeria (24°N, 8°E)

[a]Bulk Ca = insoluble + soluble Ca.

Table 8. Calcium Budget and Percentages With Respect to Bulk Ca (Soluble + Insoluble) by Provenances in Red Rains Collected at Montseny[a]

Origin	Insoluble Ca	Soluble Ca	Bulk Ca
WS (n = 13)	220 (9.1%)	2208 (91%)	2428
E (n = 10)	3143 (69%)	1420 (31%)	4563

[a]Unit is mg m^{-2}.

ones in the dust plume. It could be envisaged that finer particles (containing also carbonate particles) would be more prone to dissolution because of a higher surface to volume ratio. Thus, for more distant source areas with similar calcite content in origin, a higher soluble Ca proportion compared to bulk Ca would be expected if there was deposition of the coarser carbonates.

[42] Grain size analysis could only be performed on three samples, two from eastern provenances and one from the western one. The median particle diameter of eastern samples was 11.1 μm and 13.0 μm for the events collected on 11 and 28 March 1991, while the median diameter for the two replicated grain analysis on the western sample collected the 15 November 1999 was 7.6 μm: the eastern samples had a median diameter 32–42% higher that that of the western sample. While this result is far from conclusive because of an excessively low number of measures, the outcome is consistent with our hypothesis of coarser particles from eastern provenances.

[43] To further explore if there is particle fractionation during transport, we analyzed the relationship between CaO as representing the grain size and ^{210}Pb ($T_{1/2}$ = 22.3 yr). The comparison with ^{210}Pb is justified by the fact this earth naturally produced radionuclide is adsorbed on dust particle surfaces and can be used as a tracer of the distance traveled by dust plumes [*Marx et al.*, 2005]. Fine dust aerosols transported by air currents from the Sahara desert to the Mediterranean scavenge ^{210}Pb from the atmosphere, thus

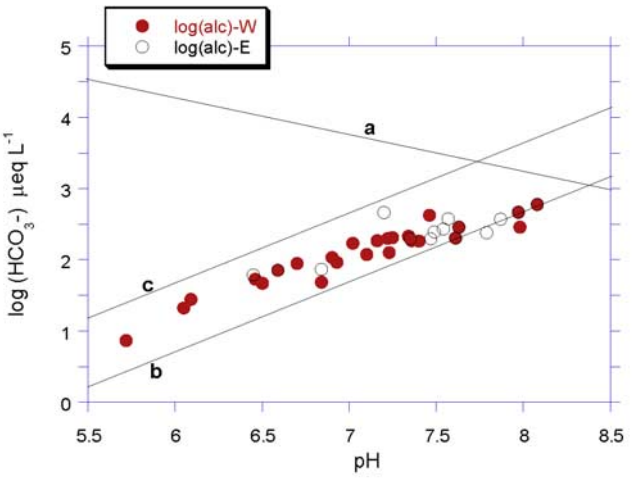

Figure 8. Relationship between HCO_3^- and pH in the filtrated red rains at Montseny distinguished by provenances. Lines show the solubility equilibrium of calcite (line a), and the carbonic acid system with pCO_2 at atmospheric concentrations (line b) and 10 times atmospheric concentrations (line c).

increasing significantly their ^{210}Pb concentration [*Garcia-Orellana et al.*, 2006]. The ^{210}Pb is attached to aerosol particles in the submicron size range (<1 μm diameter [*Winkler et al.*, 1998; *Marley et al.*, 2000]), thus in our fractionation hypothesis, the longer the transport, the higher the ^{210}Pb concentration would be. In Figure 9 the ^{210}Pb to insoluble CaO is represented. Western Saharan samples, with low insoluble CaO concentrations, have higher ^{210}Pb values (Table 5). A significant negative relationship relates both variables ($r = -0.62$; $p < 0.01$). Eastern samples lie to the high insoluble CaO side, as repeatedly observed, and have the lowest ^{210}Pb concentrations. The two variables relationship for eastern samples is not significant at $p < 0.05\%$ level ($r = -0.66$, $n = 5$). However, if we include the

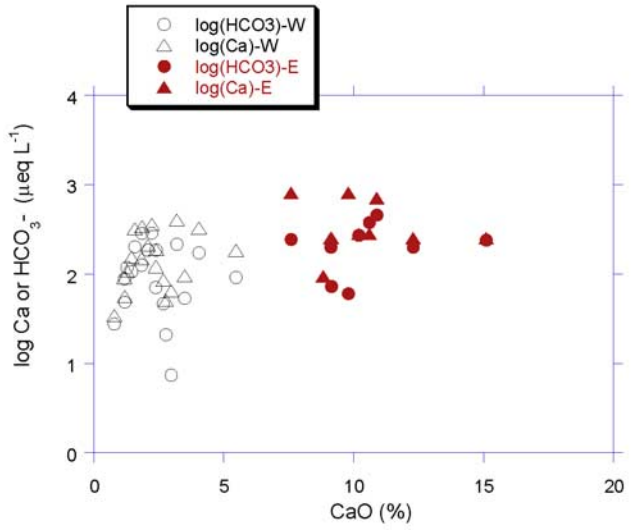

Figure 7. Relationship between the soluble products of dissolution of calcite (the ions Ca^{2+} and HCO_3^- in rain, in μeq L^{-1}, logarithmic scale) with insoluble CaO concentrations (in %) of the dust residue of red rains at Montseny.

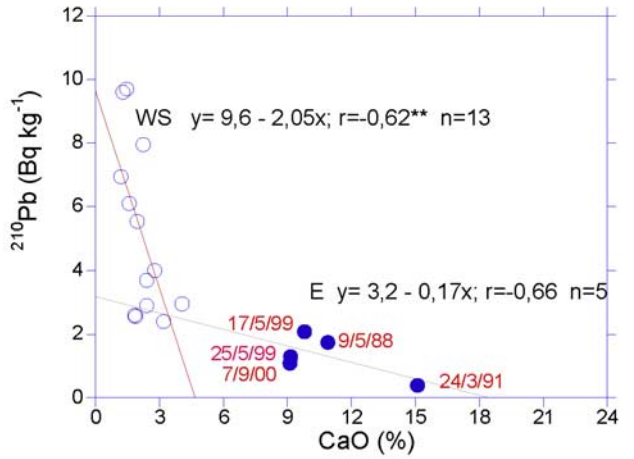

Figure 9. Relationship between ^{210}Pb concentrations and insoluble CaO concentrations in the dust residue collected in red rains at Montseny. WS and E indicate western and eastern African provenances relative to 0° Greenwich.

Table 9. Dust Deposition, Ca Content in Insoluble Phase, ^{210}Pb Concentration, and Length of Back Trajectories Distinguished by Provenances for Red Rains at Montseny in the Period 1987–2002

	Dust Deposition, mg m^{-2}	Ca, %	^{210}Pb, kBq kg^{-1}	Length
Western	971	2.2	5.15	4000
Eastern	4434	10.4	1.32	2320

Moroccan samples with the eastern group regression (to represent the relationship for events of closer provenance), the regression becomes highly significant with r increasing to -0.89 ($p < 0.001$).

[44] In Table 9 we have summarized some of the parameters that help to interpret the processes occurring during transport. It is observed that the more lengthy western trajectories deliver less insoluble material (total dust amount and insoluble Ca) than the shorter eastern trajectories to northeastern Spain during red rain episodes. Linked to this, ^{210}Pb, which is absorbed onto fine particles, is 4 times higher in western trajectories compared to the eastern ones. We propose that particle selection during transport from the west would leave the finer particles in the dust plume. These, upon interaction with the wet fronts from the Atlantic, would solubilize to a higher degree than the coarser eastern dusts because of higher surface to volume ratio in the finer western material. Also, western fluxes could have longer contact with wet fronts from the Atlantic than eastern fluxes.

[45] In order to assess the fractionation-dissolution hypothesis, more work must be done in measuring the particle diameters in red rain samples and the chemical composition by grain sizes distinguished by source areas.

5. Conclusions

[46] On the basis of back trajectories and satellite images, a distinction was made between an eastern and western air mass flux with respect to 0° Greenwich for red rain samples arriving at Montseny (northeastern Spain). Principal component and ANOVA analyses between the two provenance groups showed Ca differences in the insoluble phase, with eastern samples being significantly richer than western samples. The ratios of various elements to insoluble Ca were therefore significantly higher in western provenances. However, these differences disappeared when considering bulk Ca ratios (bulk Ca = insoluble + soluble Ca) indicating a similar total Ca at the uplifting points and therefore similar carbonated lithologies at both areas. The difference in insoluble Ca with respect to total Ca between provenances ($Ca_{insoluble}/Ca_{total}$ = 0.10 and 0.70 for western and eastern trajectories, respectively) is interpreted as a difference in calcite dissolution during transport. Evidence from ^{210}Pb data and from the length of the back trajectories indicate that western trajectories covered a longer distance than the eastern ones; their higher calcite soluble phase could be due to (1) longer contact with wet fronts from the Atlantic and (2) particle segregation during transport, with finer particles more prone to dissolution due to a higher surface to volume ratio.

[47] **Acknowledgments.** This study was financed by the Spanish Ministerio de Educación y Ciencia projects REN2001-0659/CLI, CGL2004-05984/CLI, and CGL2005-07543/CLI. The authors are grateful for the provision of the HYSPLIT transport model outputs. The authors also acknowledge the CREAF personnel for field work and Silvia Rico from Institute Jaume Almera-CSIC for work at the laboratory. The authors want to thank an anonymous reviewer for very valuable comments on earlier drafts of the manuscript.

References

Al Momani, J. F., G. Gullu, I. Olmez, U. Eler, E. Ortel, G. Sirin, and G. Tuncel (1997), Chemical composition of eastern Mediterranean aerosol and precipitation: Indication of long-range transport, *Pure Appl. Chem.*, *69*, 41–46.

Avila, A. (1996), Time trends in the precipitation chemistry at a mountain site in northeastern Spain for the period 1983–1994, *Atmos. Environ.*, *30*, 1363–1373.

Avila, A., and M. Alarcón (1999), Relationship between precipitation chemistry and meteorological situations at a rural site in NE Spain, *Atmos. Environ.*, *33*, 1663–1677.

Avila, A., and F. Rodà (1991), Red rains as major contributors of alkalinity and nutrients to a holm oak forest in the Montseny Mountains, *Orsis*, *6*, 215–229.

Avila, A., I. Queralt, and M. Alarcón (1997), Mineralogical composition of African dust delivered by red rains over north-eastern Spain, *J. Geophys. Res.*, *102*, 21,977–21,996.

Avila, A., M. Alarcón, and I. Queralt (1998), The chemical composition of dust transported in red rains: Its contribution to the biogeochemical cycle of a holm oak forest in Catalonia (Spain), *Atmos. Environ.*, *32*, 179–191.

Barkan, J., H. Kutiel, and P. Alpert (2004), Climatology of dust sources in North Africa and the Arabian Peninsula, based on TOMS data, *Indoor Built Environ.*, *13*, 407–419.

Barkan, J., P. Alpert, H. Kutiel, and P. Kishcha (2005), Synoptics of dust transportation days from Africa toward Italy and central Europe, *J. Geophys. Res.*, *110*, D07208, doi:10.1029/2004JD005222.

Bergametti, G., L. Gomes, E. Remoudaki, M. Desbois, D. Martin, and P. Buat-Ménard (1989a), Present transport and deposition patterns of African dusts to the North-Western Mediterranean, in *Paleoclimatology and Paleometeorology: Modern and Past Patterns of Global Atmospheric Transport*, edited by M. Leinen and M. Sarnthein, pp. 227–252, Springer, New York.

Bergametti, G., L. Gomes, G. Coudé-Gaussen, P. Rognon, and M. Le Costumer (1989b), African dust over Canary Islands: Source regions, identification and transport pattern for some summer situations, *J. Geophys. Res.*, *94*, 14,855–14,864.

Blanco, A., F. De Tomasi, E. Filippo, D. Manno, M. R. Perrone, A. Serra, A. M. Tafuro, and A. Tepore (2003), Characterization of African dust over southern Italy, *Atmos. Chem. Phys. Disc.*, *3*, 1–38.

Bonelli, P., G. M. Braga-Marcazzan, and E. Cereda (1996), Elemental composition and air trajectories of African dust transported in Northern Italy, in *The Impact of Desert Dust Across the Mediterranean*, edited by S. Guerzoni and R. Chester, pp. 275–283, Springer, New York.

Borbély-Kiss, I., A. Z. Kiss, E. Koltay, G. Szabó, and L. Bozó (2004), Saharan dust episodes in Hungarian aerosol: Elemental signatures and transport trajectories, *Aerosol Sci. Technol.*, *25*, 1205–1224.

Caquineau, S., A. Gaudichet, L. Gomes, M. C. Magonthier, and B. Chatenet (1998), Saharan dust: Clay ratio as a relevant tracer to assess the origin of soil delivered aerosols, *Geophys. Res. Lett.*, *25*, 983–986.

Caquineau, S., A. Gaudichet, L. Gomes, and M. Legrand (2002), Mineralogy of Saharan dust transported over northwestern tropical Atlantic Ocean in relation to source regions, *J. Geophys. Res.*, *107*(D15), 4251, doi:10.1029/2000JD000247.

Chester, R., M. Nimmo, M. Alarcón, C. Saydam, K. J. T. Murphy, G. S. Sanders, and P. Corcoran (1993), Defining the chemical character of aerosols from the atmosphere of the Mediterranean Sea and surrounding regions, *Oceanol. Acta*, *16*, 231–246.

Chiapello, I., G. Bergametti, B. Chatenet, P. Bousquet, F. Dulac, and E. Santos-Soares (1997), Origins of African dust transported over the northeastern tropical Atlantic, *J. Geophys. Res.*, *102*, 13,701–13,709.

Coudé-Gaussen, G., P. Rognon, G. Bergametti, L. Gomes, B. Strauss, J. M. Gros, and M. N. Le Coustumer (1987), Saharan dust on Fuerteventura Island (Canaries): Chemical and mineralogical characteristics, air mass trajectories and probable sources, *J. Geophys. Res.*, *92*, 9753–9771.

D'Almeida, G. A. (1986), A model for Saharan dust transport, *J. Clim. Appl. Meteorol.*, *25*, 903–916.

Draxler, R. R., and G. D. Rolph (2003), HYSPLIT (HYbrid Single-Particle Lagrangian Integrated Trajectory) Model, report, Natl. Oceanogr. Atmos. Admin., Air Res. Lab., Silver Spring, Md. (Available at http://www.arl.noaa.gov/ready/hysplit4.html)

Duce, R. A. (1986), The impact of atmospheric nitrogen, phosphorus and iron species on marine biological productivity, in *The Role of Air-Sea*

Exchange in Geochemical Cycling, edited by P. Buat-Menard, pp. 497–529, Springer, New York.

Escudero, M., S. Castillo, X. Querol, A. Avila, M. Alarcón, M. M. Viana, A. Alastuey, E. Cuevas, and S. Rodríguez (2005), Wet and dry African dust episodes over eastern Spain, *J. Geophys. Res.*, *110*, D18S08, doi:10.1029/2004JD004731.

Escudero, M., A. Stein, R. R. Draxler, X. Querol, A. Alastuey, S. Castillo, and A. Avila (2006), Determination of the contribution of northern Africa dust source areas to PM10 concentrations over the central Iberian Peninsula using the Hybrid Single-Particle Lagrangian Integrated Trajectory model (HYSPLIT) model, *J. Geophys. Res.*, *111*, D06210, doi:10.1029/2005JD006395.

Formenti, P., M. O. Andreae, L. Lange, G. Roberts, J. Cafmeyer, I. Rajta, W. Maenhaut, B. N. Holben, P. Artaxo, and J. Lelieveld (2001), Saharan dust in Brazil and Suriname during the Large-Scale Biosphere-Atmosphere Experiment in Amazonia (LBA)-Cooperative LBA Regional Experiment (CLAIRE) in March 1998, *J. Geophys. Res.*, *106*, 14,919–14,934.

Ganor, E. (1991), The composition of clay minerals transported to Israel as indicators of Saharan dust emission, *Atmos. Environ., Part A*, *25*, 2657–2664.

Ganor, E., and Y. Mamane (1982), Transport of Saharan dust across the eastern Mediterranean, *Atmos. Environ.*, *16*, 581–587.

Ganor, E., H. A. Foner, S. Brenner, E. Neeman, and N. Lavi (1991), The chemical composition of aerosols settling in Israel following dust storms, *Atmos. Environ., Part A*, *25*, 2665–2670.

Garcia-Orellana, J., J. A. Sanchez-Cabeza, P. Masqué, A. Àvila, E. Costa, M. D. Loÿe-Pilot, and J. M. Bruach-Menchén (2006), Atmospheric fluxes of ^{210}Pb to the western Mediterranean Sea and the Saharan dust influence, *J. Geophys. Res.*, *111*, D15305, doi:10.1029/2005JD006660.

Gatz, D. F., and J. M. Prospero (1980), A large silicon-aluminum aerosol plume in central Illinois: North African desert dust?, *Atmos. Environ.*, *30*, 3789–3799.

Glaccum, R. A., and J. Prospero (1980), Saharan aerosols over the tropical North Atlantic–Mineralogy, *Mar. Geol.*, *37*, 295–321.

Gillette, D. A. (1979), Environmental factors affecting dust emission by wind erosion, in *Saharan Dust*, edited by C. Morales, pp. 71–94, John Wiley, Hoboken, N. J.

Guerzoni, S., G. Quarantotto, E. Molinaroli, and G. Rampazzo (1995), More data on source signature and seasonal fluxes to the central Mediterranean Sea of aerosol dust originated in desert areas, *Water Pollut. Res. Rep.*, *32*, 267–274.

Guerzoni, S., E. Molinaroli, and R. Chester (1997), Saharan dust inputs to the western Mediterranean Sea: Depositional patterns, geochemistry and sedimentological implications, *Deep Sea Res., Part II*, *44*, 631–654.

Guieu, C., and A. J. Thomas (1996), Saharan aerosols: From the soil to the ocean, in *The Impact of Desert Dust Across the Mediterranean*, edited by S. Guerzoni and R. Chester, pp. 207–216, Springer, New York.

Guieu, C., R. Chester, M. Nimmo, J. M. Martin, S. Guerzoni, E. Nicolas, J. Mateu, and S. Keyse (1997), Atmospheric input of dissolved and particulate metals to the northwestern Mediterranean, *Deep Sea Res., Part II*, *44*, 655–674.

Guieu, C., M.-D. Loÿe-Pilot, C. Ridame, and C. Thomas (2002), Chemical characterization of the Saharan dust end-member: Some biogeochemical implications for the western Mediterranean Sea, *J. Geophys. Res.*, *107*(D15), 4258, doi:10.1029/2001JD000582.

Herman, J. R., P. K. Bhartia, O. Torres, C. Hsu, C. Seftor, and E. Celarier (1997), Global distribution of UV-absorbing aerosols from Nimbus 7/TOMS data, *J. Geophys. Res.*, *102*, 16,911–16,922.

Husar, R. B., J. Prospero, and L. L. Stowe (1997), Characterization of tropospheric aerosols over the oceans with the NOAA advanced very high resolution radiometer optical thickness operational product, *J. Geophys. Res.*, *102*, 16,889–16,909.

Jickells, T. D., et al. (2005), Global iron connections between desert dust, ocean biogeochemistry and climate, *Science*, *308*, 67–71.

Kallos, G., V. Kotroni, and K. Lagouvardos (1997), The regional weather forecasting system SKIRON: An overview, in *Proceedings of the Symposium on Regional Weather Prediction on Parallel Computer Environments*, edited by G. Kallos et al., pp. 109–122, Univ. Athens, Greece, 15–17 Oct.

Koçak, M., M. Nimmo, N. Kubilay, and B. Herut (2004), Spatio-temporal aerosol trace metal concentrations and sources in the Levantine Basin of the eastern Mediterranean, *Atmos. Environ.*, *38*, 2133–2144.

Levin, Z., and E. Ganor (1996), The effects of desert particles on cloud and rain formation in the eastern Mediterranean, in *The Impact of Desert Dust Across the Mediterranean*, edited by S. Guerzoni and R. Chester, pp. 77–86, Springer, New York.

Levin, Z., N. Price, and E. Ganor (1990), The contribution of sulfate and desert aerosols to the acidification of clouds and rain in Israel, *Atmos. Environ.*, *12*, 69–82.

Li, X., H. Maring, D. Savoie, K. Voss, and J. Prospero (1996), Dominance of mineral dust in aerosol light scattering in the North Atlantic trade winds, *Nature*, *380*, 416–419.

Löye-Pilot, M. D., and J. M. Martin (1996), Saharan dust input to the western Mediterranean: An eleven year record in Corsica, in *The Impact of Desert Dust Across the Mediterranean*, edited by S. Guerzoni and R. Chester, pp. 191–199, Springer, New York.

Löye Pilot, M. D., J. M. Martin, and J. Morelli (1986), Influence of Saharan dust on the rain acidity and atmospheric input to the Mediterranean, *Nature*, *321*, 427–428.

Marley, N. A., J. S. Gaffney, P. J. Drayton, M. M. Cunningham, K. A. Orlandini, and R. Paode (2000), Measurement of ^{210}Pb, ^{210}Po, and ^{210}Bi in size-fractionated atmospheric aerosols: An estimate of fine-aerosol residence times aerosol, *Sci. Technol.*, *32*, 569–583.

Marticorena, B., and G. Bergametti (1996), Two-year simulations of seasonal and interannual changes in Saharan dust emission, *Geophys. Res. Lett.*, *23*, 1921–1924.

Marticorena, B., G. Bergametti, D. A. Gillette, and J. Belnap (1997), Factors controlling threshold friction velocity in semiarid and arid areas of the United States, *J. Geophys. Res.*, *102*, 23,277–23,287.

Marx, S. K., B. S. Kamber, and H. M. McGowan (2005), Estimates of Australian dust flux into New Zealand: Quantifying the eastern Australian dust plume pathway using trace element calibrated ^{210}Pb as a monitor, *Earth Planet. Sci. Lett.*, *239*, 336–351.

McClain, C. R., M. L. Cleave, G. C. Feldman, W. W. Gregg, S. B. Hooker, and N. Kuring (1998), Science quality SeaWiFS data for global biosphere research, *Sea Technol.*, *39*, 10–15.

Molinaroli, E. (1996), Mineralogical characterisation of Saharan dust with a view to its final destination in Mediterranean sediments, in *The Impact of Desert Dust Across the Mediterranean*, edited by S. Guerzoni and R. Chester, pp. 153–162, Springer, New York.

Moreno, T., X. Querol, S. Castillo, A. Alastuey, E. Cuevas, L. Herrmann, M. Mounkaila, J. Elvira, and W. Gibbons (2006), Geochemical variation in aeolian mineral particles from the Sahara-Sahel Dust Corridor, *Chemosphere*, *65*, 261–270.

Moulin, C., C. E. Lambert, F. Dulac, and U. Dayan (1997), Control of atmospheric export of dust from North Africa by the North Atlantic Oscillation, *Nature*, *387*, 691–694.

Nickovic, S., G. Kallos, A. Papadopoulos, and O. Kakaliagou (2001), A model for prediction of desert dust cycle in the atmosphere, *J. Geophys. Res.*, *106*, 18,113–18,129.

Paquet, H., G. Coudé-Gaussen, and P. Rognon (1984), Etude minéralogique de poussières sahariennes le long d'un itinéraire entre 19° et 35° de latitude nord, *Rev. Geol. Dynam. Geogr. Phys.*, *25*, 257–265.

Perry, K. D., T. A. Cahill, R. A. Eldred, and D. D. Dutcher (1997), Long-range transport of North African dust to the eastern United States, *J. Geophys. Res.*, *102*, 11,225–11,238.

Prospero, J. (1996), Saharan dust transport over the North Atlantic Ocean and Mediterranean: An overview, in *The Impact of Desert Dust Across the Mediterranean*, edited by S. Guerzoni and R. Chester, pp. 133–151, Springer, New York.

Prospero, J., and T. N. Carlson (1972), Vertical and areal distribution of Saharan dust over the western equatorial North Atlantic Ocean, *J. Geophys. Res.*, *77*, 5255–5265.

Prospero, J., and T. N. Carlson (1981), Saharan air outbreaks over the tropical North Atlantic, *Pure Appl. Geophys.*, *119*, 667–691.

Prospero, J. M., P. Ginoux, O. Torres, S. E. Nicholson, and T. E. Gill (2002), Environmental characterization of global sources of atmospheric soil dust identified with the NIMBUS 7 Total Ozone Mapping Spectrometer (TOMS) absorbing aerosol product, *Rev. Geophys.*, *40*(1), 1002, doi:10.1029/2000RG000095.

Queralt-Mitjans, I., F. Domingo, and A. Solé-Benet (1993), The influence of local sources on the mineral content of bulk deposition over an altitudinal gradient in the Filabres Range (SE Spain), *J. Geophys. Res.*, *98*, 16,761–16,768.

Querol, X., A. Alastuey, A. Lopez-Soler, F. Plana, J. A. Puicercus, E. Mantilla, J. V. Miro, and B. Artiñano (1998), Seasonal evolution of atmospheric suspended particles around a coal-fired power station: Particulate levels and sources, *Atmos. Environ.*, *32*(11), 1963–1978.

Querol, X., A. Alastuey, S. Rodríguez, F. Plana, C. R. Ruiz, N. Cots, G. Massagué, and O. Puig (2001), PM_{10} and $PM_{2.5}$ source apportionment in the Barcelona metropolitan area, Catalonia, Spain, *Atmos. Environ.*, *35*, 6407–6419.

Rodríguez, S., X. Querol, A. Alastuey, G. Kallos, and O. Kakaliagou (2001), Saharan dust contributions to PM_{10} and TSP levels in Southern and E. Spain, *Atmos. Environ.*, *35*, 2433–2447.

Rodríguez, S., X. Querol, A. Alastuey, and F. Plana (2002), Sources and processes affecting levels and composition of atmospheric aerosol in the western Mediterranean, *J. Geophys. Res.*, *107*(D24), 4777, doi:10.1029/2001JD001488.

Rosenfeld, D., and I. Lensky (1998), Satellite-based insights into precipitation formation processes in continental and maritime convective clouds, *Bull. Am. Meteorol. Soc.*, *79*, 2457–2476.

Sanchez-Cabeza, J. A., P. Masqué, and I. Ani-Ragolta (1998), ^{210}Pb and ^{210}Po analysis in sediments and soils by microwave acid digestion, *J. Radioanal. Nucl. Chem.*, *227*, 19–22.

Schütz, L. (1989), Atmospheric mineral dust. Properties and source markers, in *Paleoclimatology and Paleometeorology: Modern and Past Patterns of Global Atmospheric Transport*, edited by M. Leinen and M. Sarnthein, pp. 359–383, Springer, New York.

Sokolik, I. N., O. B. Toon, and R. W. Bergstrom (1998), Modeling the radiative characteristics of airborne mineral aerosols at infrared wavelength, *J. Geophys. Res.*, *103*, 8813–8826.

Stumm, W., and J. J. Morgan (1981), *Aquatic Chemistry*, 2nd ed., 780 pp., John Wiley, Hoboken, N. J.

Stuut, J.-B., M. Zabel, V. Ratmeyer, P. Helmke, E. Schefuß, G. Lavik, and R. Schneider (2005), Provenance of present-day eolian dust collected off NW Africa, *J. Geophys. Res.*, *110*, D04202, doi:10.1029/2004JD005161.

Swap, R. M., M. Garstang, S. Greco, R. Talbot, and P. Kallberg (1992), Saharan dust in the Amazon basin, *Tellus, Ser. B*, *44*, 133–149.

Swap, R., S. Ulanski, M. Cobbett, and M. Garstang (1996), Temporal and spatial characteristics of Saharan dust outbreaks, *J. Geophys. Res.*, *101*, 4205–4220.

Taylor, S. R., and S. M. McLennan (1985), *The Continental Crust: Its Composition and Evolution*, edited by A. Hallum, 312 pp., Blackwell Sci., Malden, Mass.

Tegen, I., A. A. Lacis, and I. Fung (1996), The influence on climate forcing of mineral aerosols from disturbed soils, *Nature*, *280*, 419–422.

Viana, M., X. Querol, A. Alastuey, E. Cuevas, and S. Rodríguez (2002), Influence of African dust on the levels of atmospheric particulates in the Canary Islands air quality network, *Atmos. Environ.*, *36*, 5861–5875.

Westphal, D. L., O. B. Toon, and T. N. Carlson (1987), A two dimensional numerical investigation of the dynamics and microphysics of Saharan dust storms, *J. Geophys. Res.*, *92*, 3027–3049.

Winkler, R., F. Dietl, G. Frank, and J. Tschiersch (1998), Temporal variation of ^{7}Be and ^{210}Pb size distributions in ambient aerosol, *Atmos. Environ.*, *32*, 983–991.

M. Alarcón, Departament de Física i Enginyeria Nuclear, Universitat Politècnica de Catalunya, Av. Víctor Balaguer, s/n, E-08800 Vilanova i La Geltrú, Spain.

A. Avila, Centre de Recerca Ecològica i Aplicacions Forestals, Universitat Autònoma de Barcelona, E-08193 Bellaterra, Spain.

S. Castillo, M. Escudero, and X. Querol, Institut Jaume Almera, Consejo Superior de Investigaciones Científicas, Solé Sabarís, s/n, E-08028 Barcelona, Spain.

J. García Orellana and P. Masqué, Institut de Ciència i Tecnologia Ambientals, Departament de Física, Universitat Autònoma de Barcelona, E-08193 Bellaterra, Spain.